

# On the topology of synchrony optimized networks of a Kuramoto-model with non-identical oscillators

David Kelly and Georg A. Gottwald

*School of Mathematics and Statistics, University of Sydney, New South Wales 2006, Australia*

(Received 31 January 2011; accepted 25 April 2011; published online 28 June 2011)

We study synchrony optimized networks. In particular, we focus on the Kuramoto model with non-identical native frequencies on a random graph. In a first step, we generate synchrony optimized networks using a dynamic breeding algorithm, whereby an initial network is successively rewired toward increased synchronization. These networks are characterized by a large anti-correlation between neighbouring frequencies. In a second step, the central part of our paper, we show that synchrony optimized networks can be generated much more cost efficiently by minimization of an energy-like quantity  $E$  and subsequent random rewires to control the average path length. We demonstrate that synchrony optimized networks are characterized by a balance between two opposing structural properties: A large number of links between positive and negative frequencies of equal magnitude and a small average path length. Remarkably, these networks show the same synchronization behaviour as those networks generated by the dynamic rewiring process. Interestingly, synchrony-optimized network also exhibit significantly enhanced synchronization behaviour for weak coupling, below the onset of global synchronization, with linear growth of the order parameter with increasing coupling strength. We identify the underlying dynamical and topological structures, which give rise to this atypical local synchronization, and provide a simple analytical argument for its explanation. © 2011 American Institute of Physics.  
[doi:10.1063/1.3590855]

**Synchronization of networks is a ubiquitous phenomenon. The Kuramoto model describing the interaction of a network of identical oscillators has attracted mathematical interest because of its analytical tractability. In this paper, we will study the Kuramoto model with non-identical oscillators. An important question is how a network should be organized to allow for optimal synchronization behaviour of the oscillators. Several computational methods have been recently introduced to establish synchrony optimized networks, based on dynamic rewiring<sup>5,6</sup> and simulated annealing.<sup>9,8</sup> However, these methods, although successful, are computationally extremely costly and prohibit the study of large networks. In this paper, we will propose a very simple and cheap algorithm to create synchronization optimized networks.**

Given the good synchronization properties of small world networks,<sup>27</sup> which are characterized by a high clustering coefficient and a small average path length, it was long believed that a small average path length assures good synchronization behaviour. Small path length has been associated with heterogeneity in degree distribution.<sup>7</sup> It has since been shown, however, that some homogeneity in the degree distribution is actually desirable when optimizing for synchrony at the expense of small average path length.<sup>22,20</sup> The notion of homogeneity in the context of synchronization has been pushed further by so called entangled networks, which are synchrony optimized<sup>9</sup> and exhibit large girth and homogeneous degree, betweenness, and distance distributions.

Prompted by these findings, research has turned away from testing individual structural traits, instead focussing on finding a collection of structural properties that fit together in a network constructively, with the aim of optimizing synchronizability.<sup>5,9</sup> This can be achieved by making small mutations consisting of rewirings to a given network and accepting those mutations which make a network fitter for synchronization. By tracking the structural properties over the course of the evolution, one can identify the emergence of those properties that together constitute the synchrony optimal topology.

We follow this trend of seeking the optimal topology, but without the common assumption that all oscillators are intrinsically identical.<sup>9,20,22,23</sup> In Refs. 5 and 6, a dynamical rewiring procedure was introduced to optimize synchronization at a particular coupling strength. The algorithm rewires a given network in order to maximize the level of phase

## I. INTRODUCTION

The notion of complex networks is a powerful way to describe and understand the collective behaviour of many interacting agents. Applications range from biology, neurophysiology, and social behaviour to technological examples such as electric power grids and the Internet.<sup>26,21,4</sup> Recently, much attention has been paid to the interplay between the structure or topology of the network and the dynamics that takes place on the network. This is particularly important in the problem of mutual synchronization of oscillators. The question we ask in this work is “What are the properties of a network that are optimal with respect to synchronization?”

coherence measured by a synchronization order parameter. By tracking the evolution of topological properties of the network over the course of the rewiring process, it was found that synchrony optimized networks are characterized by a prevalence of connections between nodes with similar magnitudes of native frequencies but opposite signs. The networks found in Ref. 5 exhibited a significant drop in the average path length during the final stages of the optimization procedure. This was linked in Ref. 5 to the formation of hubs. As discussed above, the creation of hubs is in some cases detrimental for synchronization.<sup>22,20</sup> We will therefore modify the dynamic rewiring algorithm (DRA) proposed in Ref. 5 to allow only for rewirings, which preserve the initial degree distribution.

We will then introduce an energy-like quantity  $E$ , which measures the correlation of frequencies with the same magnitude but opposite signs and will construct network topologies that minimize this energy. We present an efficient and straightforward algorithm to generate those  $E$ -minimized networks. The average path length of those networks is much larger than the one associated with DRA-synchrony-optimized networks or with an Erdős-Rényi network with the same number of nodes and the same mean degree. The increased path length is reflected in an overall poorer synchronization behaviour of global synchronization. We therefore, akin to the idea of the small-world network, propose a rewiring algorithm to the  $E$ -minimized network. We demonstrate that approximate synchrony optimized networks are given as a balance between requiring small average path length and assuring homogeneity in the sense of how native frequencies are distributed over the network.

Interestingly, we will see that synchrony-optimized networks exhibit significantly enhanced synchronization behaviour for weak coupling strength, below the onset of global synchronization. We coin this *local synchronization*. In this regime, the order parameter is a linear function of the coupling strength. We will explain this atypical behaviour by investigating local interactions of partially synchronized clusters.

The paper is organized as follows. In the following section, we describe the networks under consideration and introduce order parameters to measure synchronization. In Sec. III, we describe the methods to generate synchrony optimized networks. We introduce two methods, a modification of the dynamic rewiring algorithm (DRA) developed in Ref. 5 and a novel algorithm based on a minimization procedure of an energy-like quantity with subsequent random rewirings to ensure sufficiently small average path length. These synchrony-optimized networks not only exhibit the well known global synchronization at large coupling strength but also local synchronization at weak coupling strength. This will be analyzed in Sec. IV. We conclude in Sec. V with a discussion.

## II. THE MODEL

We will study the Kuramoto model for  $N$  phase oscillators  $\phi_i$  with non-identical native frequencies  $\omega_i$ . The Kuramoto model is a simple paradigmatic model for synchronization phenomena<sup>25,1,2</sup> and is written as

$$\dot{\phi}_i = \omega_i + \frac{K}{N} \sum_{j=1}^N a_{ij} \sin(\phi_j - \phi_i), \quad (2.1)$$

where the natural frequencies  $\omega_i$  are randomly chosen from a uniform distribution  $\mathcal{U}(-1, 1)$ . The adjacency matrix  $\mathbb{A} = \{a_{ij}\}$  determines the topology of the network and describes which oscillators are connected. For interacting oscillators, generically, there exists a critical coupling strength  $K_c$  such that, for sufficiently large coupling strength  $K > K_c$ , the oscillators synchronize in the sense that they become locked to their mutual mean frequency and their phases become localized about their mean phase.<sup>24,3</sup> This type of synchronous behaviour known as global synchronization occurs if the dynamics settles on a globally attracting manifold.

We restrict our analysis to unweighted, undirected networks for which the adjacency matrix  $\mathbb{A} = \{a_{ij}\}$  is symmetric with  $a_{ij} = a_{ji} = 1$  if there is an edge between oscillators  $i$  and  $j$  and  $a_{ij} = 0$  otherwise. As in our initial network from which we start our synchrony optimization we choose connected Erdős-Rényi random graphs (ERs), characterized by a parameter  $p \in (0, 1)$ , which describes the likelihood of an edge joining two nodes (or oscillators). ERs feature a small average path length  $\ell$  which scales only logarithmically with the size  $N$  of the network as  $\ell \simeq \log(N)/\log(\langle k \rangle)$  with the mean degree  $\langle k \rangle = \sum_i \deg(i)/N = p(N-1)$  and a Poisson degree distribution.

In the following, we will study how the adjacency matrix, and hence the topology of the network, has to be constructed to allow for an optimal communication between the oscillators leading to partial and/or global synchronization. Synchronization is usually monitored via the order parameter

$$r(t) = \frac{1}{N} \left| \sum_{j=1}^N e^{i\phi_j(t)} \right|, \quad (2.2)$$

with  $0 \leq r \leq 1$ . The asymptotic limit of this order parameter can be estimated by introducing

$$\bar{r} = \lim_{T \rightarrow \infty} \frac{1}{T} \int_{T_0}^{T_0+T} r(t) dt, \quad (2.3)$$

where  $T_0$  is chosen large enough to eliminate any possible transient behaviour of the oscillators. The order parameter  $r$  and its long time average  $\bar{r}$  provide a measure for phase coherence. That is, full synchronization as measured by  $r$  is defined as  $\phi_i(t) = \phi_j(t)$  for all pairs  $i, j$  and for all times  $t$ . The order parameter  $\bar{r} \approx 1$  indicates complete synchronization, and  $\bar{r} = \mathcal{O}(1/\sqrt{N})$  indicates incoherent phase dynamics; values inbetween indicate partial coherence.

In the following, we will discuss methods, which are designed to evolve a network toward enhanced synchrony as measured by  $\bar{r}$ .

## III. SYNCHRONY OPTIMIZED NETWORKS

Studying how to optimally rewire networks is an ongoing problem. The fully synchronized state can be studied by means of the master stability function approach<sup>23</sup> and is

determined by the ratio of the largest nonzero eigenvalue and the smallest eigenvalue of the Laplacian matrix. This has been used to study given networks as well as to design rewiring strategies of networks.<sup>22,20,9,11,12,14</sup> We will apply here schemes, which have a less rigorous foundation but allow us to evolve networks, which are not yet fully synchronized. Synchrony here is measured by means of the order parameter  $\bar{r}$  defined in Eq. (2.3). This includes the fully synchronized state as well as partially synchronized states.<sup>11,12,6,28</sup>

## A. DRA

In a recent paper,<sup>5</sup> a method was proposed based on a rewiring algorithm designed to optimize synchronization at a specified coupling strength  $K = K^*$ . The measure for synchronization used is  $\bar{r}$ , although combinations of  $\bar{r}$  and local order parameters have been used as well.<sup>6</sup> This approach allows one to study the network topology and structure even at coupling strengths before full synchronization has been achieved. We will follow<sup>5</sup> and briefly describe how we apply it: Given an initial network with a specified initial structure  $\{a_{ij}\}$  and distribution of frequencies (we choose the frequencies from a uniform distribution  $\mathcal{U}(-1, 1)$ ), the initial conditions  $\phi_i(0)$ , drawn from a normal distribution with unit variance, are evolved using the Kuramoto model [Eq. (2.1)] at some fixed coupling strength  $K^*$ . The network is then successively rewired for fixed  $K = K^*$ , thereby changing the network structure, to achieve enhanced synchronization measured by higher values of  $\bar{r}(K^*)$  for the rewired networks. The order parameter  $\bar{r}(K^*)$  is determined after each rewiring through a sufficiently long simulation of the Kuramoto model [Eq. (2.1)]. A rewiring is accepted if the value of  $\bar{r}$  is larger compared with the value obtained from the previous network structure. The synchrony optimized network is then obtained once  $\bar{r}$  reaches a stationary value after successive rewirings. The actual optimization is performed at one fixed  $K^* > K_c$ . The resulting synchrony optimized network is then simulated for a range of coupling strength  $K$  to obtain the corresponding  $\bar{r}(K)$ -curve.

We modify the method described in Ref. 5 and allow only those rewirings, which preserve the degree distribution to isolate those structural network properties not related to the creation of hubs, which may prohibit synchronization.<sup>20,22</sup> This is achieved by employing the Maslov-Sneppen rewiring algorithm<sup>19</sup> rather than a random edge-replacement as done in Refs. 5 and 9. In the Maslov-Sneppen algorithm, two unconnected edges connecting four distinct nodes are randomly drawn, and then mutually rewired, provided the rewiring leaves the network connected and does not create self-loops or double edges.

In our numerical simulations, we use as an initial network an Erdős-Rényi random graph specified by the number of nodes  $N$  and the mean degree  $\langle k \rangle$ . We chose here  $N = 500$  and  $\langle k \rangle = 25$ . The coupling strength  $K^*$ , at which the optimization procedure is performed at, is chosen as  $K^* = 30$  so that  $\bar{r}(K^*) \approx 0.9$  for this initial network, which allows the optimization to be performed on a network that is already close to synchronization. To determine  $\bar{r}$ , we eliminate transient behaviour by choosing an appropriate  $T_0$  and time win-

dow  $T$  in which to perform the temporal average [Eq. (2.3)]. In particular, we used  $T_0 = 50$  and  $T = 100$  for networks with  $N = 500$  oscillators for which the value of  $\bar{r}$  has converged. The rewiring is terminated if the number of consecutive rejected rewirings exceeds twice the number of edges  $N_{\text{edges}} = 1/2 \sum_i \text{deg}(i) = 1/2 \sum_{i,j} a_{ij}$ .

In Figure 1, we show the order parameter  $\bar{r}$  as a function of the coupling strength  $K$  for the initial network and for the synchrony optimized network created by the dynamic rewiring as described above. One can clearly see the enhanced synchrony for all values of  $K$  and not just for  $K^*$  at which the optimization was performed. Both networks exhibit global synchronization for sufficiently large values of the coupling strength  $K > K_c$  with the onset of global synchronization being significantly smaller for the DRA-synchrony optimized networks at  $K_c \approx 18$  compared to  $K_c \approx 25$  for the initial ER. To estimate the value of  $K_c$ , we use the inflection point of the  $\bar{r}$ -curve as a rough measure. We note that for sufficiently large coupling strengths, the initial ER network will also reach full synchronization with  $\bar{r} \approx 1$ . Typically, one expects to see non-synchronous behaviour for weak coupling strength  $K < K_c$ , followed by the sudden onset of the global synchrony branch for  $K > K_c$ . This behaviour is evident in the initial ER network illustrated in Figure 1. Surprisingly, the DRA-networks show enhanced synchronization below the onset of global synchronization for  $K < K_c$ . A remarkable feature is the observed atypical linear dependency of  $\bar{r}$  on  $K$  below the onset of global synchronization. We label this the *local synchrony regime*. In previous work on synchrony-optimized networks, this regime had not been observed, and indeed for smaller networks this regime is not apparent in DRA networks (see figures in Ref. 5). We shall explain the presence of the local synchrony branch and detail the mechanisms behind this atypical behaviour in Sec. IV.

When using DRA one has to bear in mind the following caveats. The DRA approach is only designed to find local maxima and may in principle miss the global maximum. However, we have tested that for initial networks at sufficiently strong coupling strengths above the critical value of the initial ER, using  $K^* > 25 \approx K_c$ , the optimized network and the associated topological properties are robust. We found that for  $K^* = 30$ , where  $\bar{r} \approx 0.9$  the optimization

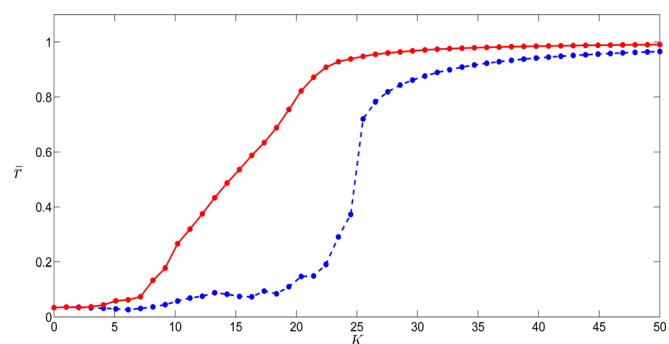


FIG. 1. (Color online) Synchrony order parameter  $\bar{r}$  as a function of coupling strength  $K$  for the  $N = 500$  initial random ER network (dashed line, online blue) and for the synchrony optimized version of the same network using the approach detailed in Sec. III A (continuous line, online red). The DRA synchrony optimization was performed at  $K^* = 30$ .

converges fastest toward the global maximum defined by the globally attracting synchronization manifold. If the dynamics is not attracted to a globally attracting set (i.e., in particular for  $K^* < K_c \approx 25$ ), the DRA procedure shows dependence on the initial conditions  $\phi_i(0)$ . For coupling strengths  $K < K_c$ , we found DRA unable to optimize the networks to significant values of  $\bar{r}$  suggesting the algorithm is finding only a local maximum.

Note that the DRA approach relies obviously on the definition of synchronizability via the choice of the order parameter  $\bar{r}$  with respect to which the optimization is performed. One may think of optimizing not  $\bar{r}$  for one particular  $K^*$  but rather optimizing networks by minimization of the onset of global synchronization  $K_c$ . However, this would be computationally much more expensive and would require finite size scaling (e.g., Ref. 15). There is, however, numerical evidence that the two approaches are equivalent if  $K^*$  is chosen sufficiently large. In Ref. 5, it was shown that for sufficiently large  $K^*$ , the optimized networks had larger values of  $\bar{r}$  for all coupling strengths, implying an earlier onset of synchronization. To show that the two approaches are equivalent and to find for which optimization schemes this is the case is a non-trivial matter, which we do not attempt to address here. We have checked numerically, however, that the topological properties of DRA-optimized networks and the  $\bar{r}(K)$ -curves are invariant if initialized at different values of  $K^*$  provided  $K^* > K_c \approx 25$ , suggesting that  $K_c$  is minimized as well.

## B. Topological structure of DRA-optimized networks

We now look in detail at the topological structure of DRA-optimized networks. To understand what structural properties we can associate with enhanced synchrony, we plot in Figure 2 how certain parameters change during the optimization process. In particular, we look at the average path length  $\ell$  defined as

$$\ell = \frac{1}{\frac{1}{2}N(N+1)} \sum_{i \geq j} d_{ij},$$

where  $d_{ij}$  is the shortest path length between nodes  $i$  and  $j$ . Note that  $d_{ij}$  is finite in connected networks. We further analyze the clustering coefficient (or transitivity)

$$C = \frac{3 \times \text{number of triangles in the network}}{\text{number of connected triples of vertices}},$$

which measures the heightened probability of two neighbours of a node sharing an edge. It measures the triangle density of the network, where the factor of 3 in the numerator takes into account that each triangle contributes three connected triples. In ER's, the connectivity is given by  $C = \langle k \rangle / (N - 1)$ . In Ref. 5, the following two parameters turned out to be of utmost importance for synchrony optimized networks, the frequency sign ratio  $p_-$ , which measures the proportion of edges linking oscillators, whose native frequency has the opposite sign, and the correlation coefficient  $c_\omega \in [-1, 1]$  defined as

$$c_\omega = \frac{\sum_{i,j} a_{ij}(\omega_i - \langle \omega \rangle)(\omega_j - \langle \omega \rangle)}{\sum_{i,j} a_{ij}(\omega_i - \langle \omega \rangle)^2}, \quad (3.1)$$

which measures the correlation between frequencies of adjacent nodes and quantifies how likely nodes with large positive native frequencies are connected to nodes with large negative native frequencies.

In Figure 2, it is seen that synchrony optimized networks are characterized by a low clustering coefficient, strongly negative values of  $c_\omega$ , and large values of  $p_-$ . Therefore, the optimized network no longer exhibits the structural properties of an ER. We note that, contrary to the results presented in Ref. 5, the average path length  $\ell$  increases rapidly albeit slightly in the later stages of the optimization. This counter-intuitive result along with the low clustering coefficient is in line with the idea of homogeneity promoted in Refs. 22, 20, and 9. Note that although large values of the correlation coefficient  $c_\omega$  and large clustering coefficients have each been identified as individually promoting synchronizability,<sup>10</sup> these are incommensurate properties in the networks

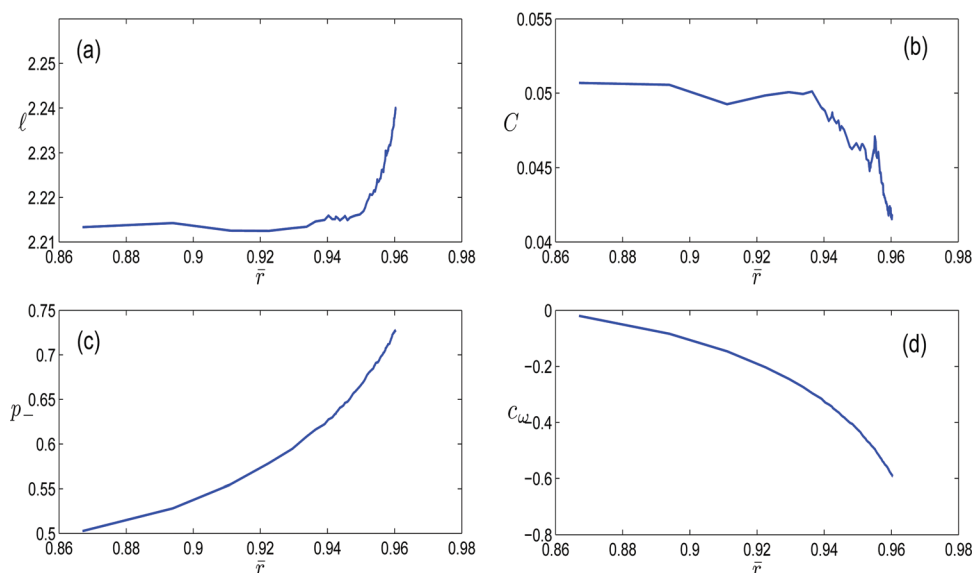


FIG. 2. (Color online) Change of structural network parameters during the DRA optimization process. The lowest value of  $\bar{r}$  refers to the initial random network and the largest value of  $\bar{r}$  to the final synchrony optimized network. (a) Average path length  $\ell$ , (b) clustering coefficient  $C$ , (c) frequency sign ratio  $p_-$ , and (d) frequency correlation  $c_\omega$ . We used an initial ER with  $N = 500$  nodes and  $\langle k \rangle = 25$ , and initialized the DRA optimization at  $K^* = 30$ .

we consider: Triangles are a poor configuration for maximizing anti-correlation, because they must contain a plus-plus or minus-minus pair. Therefore, the optimal network contains very few triangles, explaining the drop in clustering coefficient from the value of the initial ER network with  $C = \langle k \rangle / (N - 1) = 0.05$  observed in Figure 2(a).

The results for  $c_\omega$  and  $p_-$  suggest a different type of homogeneity in synchrony optimized networks with non-identical native frequencies: the nodes are arranged in such a way as to maximize the ratio of positive-negative pairs of native frequencies as well as their anti-correlation. This allows strongly positive and strongly negative native frequencies to neutralize toward the mean frequency  $\langle \omega \rangle = 0$ . It is this tendency of synchrony optimized networks to form linear structures of positive-negative native frequency node pairs, which is responsible for the increase in path length.

### C. $E$ -networks

The results from Ref. 5 for random rewirings and our own results for degree-preserving rewirings described in Sec. III B suggest that for Kuramoto-models with non-identical oscillators, synchrony optimized networks are characterized by a strong anti-correlation of adjacent positive and negative native frequencies. In light of these results, we propose to reformulate the optimization of synchrony as an optimization problem for certain structural network properties. Analogously to spin systems, we define an “energy”

$$E = \frac{1}{2} \Omega \Lambda \Omega^T, \quad (3.2)$$

where the frequency vector  $\Omega$  is defined as  $\Omega = (\omega_1, \omega_2, \dots, \omega_N)$ . Note that the energy  $E$  is just a (non-normalized) reformulation of the frequency correlation coefficient  $c_\omega$  (compare with Eq. (3.1)). For frequency distributions with non-zero mean of the native frequencies  $\langle \omega \rangle$ , we simply replace  $\Omega$  by  $\Omega - \langle \omega \rangle$ .

The results of Sec. III B suggest to minimize this energy. This can be done by iteratively pairing up the nodes occupied by negative native frequencies of largest absolute values with the available nodes occupied by positive native frequencies with largest absolute value. This is achieved efficiently by a shoestring method, as seen in Figure 3. To generate  $E$ -minimized networks one starts with an edge-free network, keeping note of each node degree. The first edge is then chosen between those two nodes which contribute the maximal negative energy. The second edge is chosen to be the edge which contributes the second most negative energy, provided the two nodes concerned each have a vacant degree. This is repeated until all nodes have reached their initial fixed node degree. This iterative algorithm, however, fails when there are only two nodes left and no further edges can be laid without creating multiple edges between these two nodes. We bypass this problem by simply stopping the algorithm at this point and leaving out these extra edges. In most networks, we consider around 20 edges out of 6250 are omitted, which has minimal effect on the synchronizability and topological properties of the optimized network.

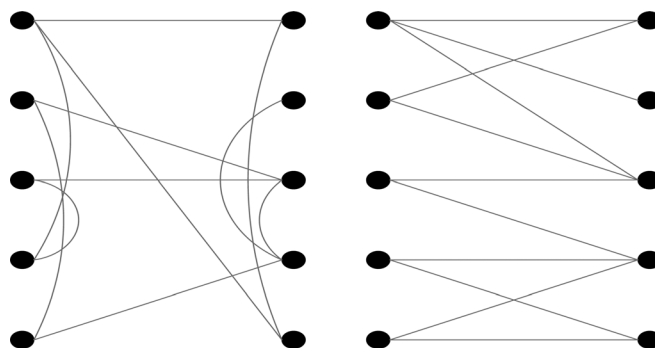


FIG. 3. Illustration of networks of minimal energy  $E$ . Left: Initial ER with  $N = 10$  nodes. Nodes with positive frequencies are on the right and nodes with negative frequencies on the left. Nodes are ordered from top to bottom with decreasing absolute value of their frequencies. Right: The same network but rewired to minimize  $E$ .

Minimizing the energy  $E$  creates a particular network structure. The energy  $E$  measures correlation of adjacent native frequencies. So by minimizing  $E$ , nodes with  $\omega_i > 0$  will, with high probability, be linked to nodes  $\omega_j < 0$  with similar magnitude. This creates an approximate bipartition in the network, where nodes are divided into camps of positive and negative  $\omega_i$ . In Figure 3, we compare a typical  $E$ -minimized network with its corresponding initial ER with  $N = 10$  nodes and mean degree  $\langle k \rangle = 2.2$ . One clearly sees how nodes of similar  $|\omega_i|$  but opposite sign are paired together in the  $E$ -minimized network. This community structure is not present in the DRA network to the same extent.

The synchronization behaviour of energy-minimized networks is illustrated in Figure 4. The order parameter  $\bar{r}$  is shown as a function of the coupling strength for a 500-node network obtained by minimizing  $E$  and compared to the DRA synchrony-optimized network. The onset of global synchronization is delayed with  $K_c \approx 27$  for the  $E$ -minimized network and  $K_c \approx 18$  for DRA. The values of  $\bar{r}$  of the DRA-optimized network are significantly larger than for the  $E$ -minimized network for most values of  $K$ . For very large coupling strengths  $K \gg K_c$ , both network types exhibit similar synchronization behaviour (not shown), as expected. However, for very small values of the coupling strength  $K$ ,  $E$ -minimized networks are superior.

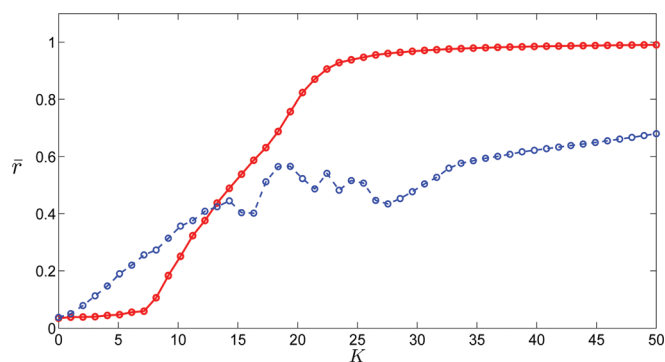


FIG. 4. (Color online) Synchrony order parameter  $\bar{r}$  as a function of coupling strength  $K$  for optimal networks with  $N = 500$  nodes and mean degree  $\langle k \rangle = 25$  produced by the dynamic approach (DRA) (continuous line, online red) and by minimizing  $E$  (dashed line, online blue). We used an average over six  $E$ -minimized networks generated from different initial ER networks with same  $N$  and mean degree.

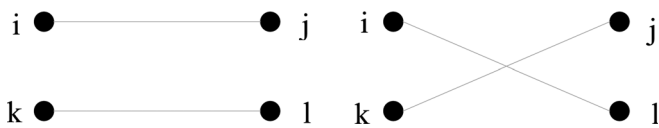


FIG. 5. Sketch of the rewiring. The nodes with negative native frequencies are on the left hand side and the nodes with positive native frequencies on the right hand side.

Let us now investigate the cause for this overall poor synchronization behaviour of  $E$ -minimized networks. The energy of the DRA-optimized network with  $E = -1614$  is much smaller in absolute value than the minimal energy of the  $E$ -minimized network with  $E_{\min} = -2008$ . However, the reader may have already suspected that the “shoestring” nature of the edges in the approximate bipartite  $E$ -minimized networks implies a much larger average path length  $\ell$  than for an ER of equal size. A path from a node of  $\omega_i > 0$  to a node of  $\omega_j > 0$  must go via a node of  $\omega_k < 0$ , thus, paths between nodes of the same sign are of length 2, 4, 6, and so forth. Similarly, paths between non-adjacent nodes of opposite sign are of length 3, 5, 7, and so forth. This bipartition then implies an increase in the average path-length of the network, making it difficult for frequency information to propagate and hence harder to reach a state of global synchronization. The delayed onset of global synchronization of  $E$ -minimized networks and their significantly reduced global synchronizability,<sup>6,10,13</sup> reflected by the lower values of  $\bar{r}$  for large coupling strengths  $K > K_c$ , can be linked to a massively increased average path length. The DRA-optimized networks have an average path length of  $\ell = 2.34$ , which is close to the theoretical value of a corresponding ER with  $\ell_{ER} \simeq \log(N)/\log(\langle k \rangle) = 1.93$ . The  $E$ -minimized network, however, exhibits a large average path length  $\ell = 6.14$ . Furthermore, the bipartite structure leads to a clustering of nodes with large absolute values of their native frequencies  $|\omega_i|$ . We have checked that those large- $|\omega_i|$  neighbourhoods are highly resistant to entrainment even at large coupling strengths.

The reader will have noticed in Figure 4 that the synchronization behaviour at moderate values of the coupling strength  $K$  in  $E$ -minimized networks is not monotonically increasing as is the case for the global synchrony branch. This can be attributed to deconstructive interference between two separate clusters of synchronous oscillators. Detailed analysis of this and other phenomena present in minimal energy networks will be presented elsewhere.<sup>17</sup>

#### D. $(E, \ell)$ -networks

To control the increase of the average path length  $\ell$  associated with the approximate bipartite structure of the  $E$ -minimized network, we propose the following random rewiring, inspired by the small world networks.<sup>27</sup>

As with the Maslov-Sneppen rewiring procedure,<sup>19</sup> we choose two edges  $(i, j)$  and  $(k, l)$  of an  $E$ -minimized network and rewire them as depicted in Figure 5, accepting the rewiring with probability

$$P(i, j, k, l) = \min\{\exp(-q|\omega_i - \omega_l|^2), \exp(-q|\omega_j - \omega_k|^2)\}.$$

The rewiring procedure is repeated until  $E$  and  $\ell$  have reached constant values. We coin those networks  $(E, \ell)$ -networks. The procedure produces approximately anti-diagonal networks, whose adjacency matrices are now supported by a Gaussian distribution centred on the anti-diagonal (provided the native frequencies are ordered according to their values with  $\omega_1 < \omega_2 < \dots < \omega_N$ ). We show in Figure 6 the adjacency matrix  $\mathbb{A}$  for a 500-node network for several values of  $q$ . The value  $q = \infty$  corresponds to the original  $E$ -minimized network because the probability of a rewiring is zero. The adjacency matrix has a clear anti-diagonal structure. At the other extreme, the value  $q = 0$  corresponds to ER when all rewirings will be accepted. For sorted native frequencies which are uniformly distributed,  $1/\sqrt{q}$  is the characteristic width of the anti-diagonal.

In Figure 7, we show how the energy  $E$  and the average path length  $\ell$  change as a function of  $q$ . For  $q \ll 1$ , the network is Erdős-Rényi-like and has  $|E|/|E_{\min}| \ll 1$  and  $\ell \approx \ell_{ER} \simeq \log(N)/\log(\langle k \rangle) = 1.93$ . For large values of  $q$ , the network will stay close to the energy-minimized network with  $E \approx E_{\min} = -2008$  and a corresponding large average path length  $\ell = 6.14$  (not shown).

For large  $q$ , i.e., close to the  $E$ -minimized state, we can estimate the average path length  $\ell$  as a function of  $q$ . Due to the approximate anti-diagonal structure of the adjacency matrix, the path length can be estimated by the average width  $W$  of the anti-diagonal band (see Figure 6) as  $\ell \sim N/W$ . Since the width of the band is given by  $W \sim 1/\sqrt{q}$ , we obtain

$$\ell - \ell_{ER} \sim \sqrt{q}.$$

This is numerically verified in Figure 8. For very large values of  $q$ , when  $\ell$  saturates to the average path length of

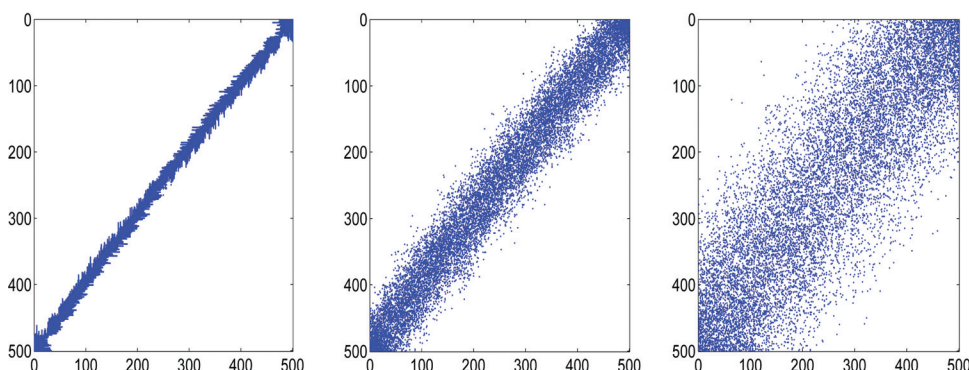


FIG. 6. (Color online) Visual representation of the adjacency matrix  $\mathbb{A}$  of  $N = 500$  node  $(E, \ell)$ -networks for different values of  $q$ . Here, we assume the node indices are sorted by decreasing native frequency. Entries with  $a_{ij} = 1$  are coloured dark (online blue). Left:  $E$ -minimized network with  $q = \infty$ . Middle:  $q = 30$ . Right:  $q = 5$ .

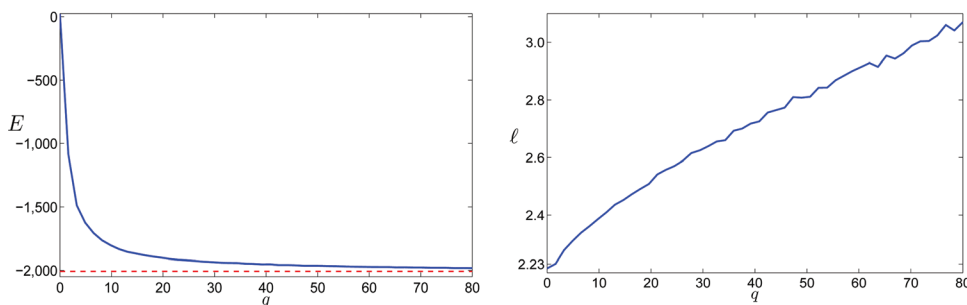


FIG. 7. (Color online) Energy  $E$  and path length  $\ell$  as a function of the rewiring probability  $q$ . The red dashed line represents the energy of the  $E$ -minimized network.

the  $E$ -minimized network, and for very small values of  $q$ , when  $W > N$ , the formula is obviously not correct, but it captures the behaviour of the average path length for a large range of  $q$ .

The above discussion suggests that the dominant structural and topological properties of synchrony optimized networks are the energy  $E$  and the average path length  $\ell$ . We now show that synchrony-optimized networks are characterized by a trade-off between small energies  $E$  and small average path length  $\ell$ . We can find a range of values  $q^*$  for which the resulting  $(E, \ell)$ -networks exhibit the same synchronization behaviour as DRA optimized networks. In Figure 9, we show the order parameter  $\bar{r}$  as a function of coupling strength  $K$  for the DRA-optimized network and for  $(E, \ell)$ -networks with  $q = 0$  (equivalent to ER),  $q = \infty$  (equivalent to  $E$ -minimized network), and for  $q = 30$ . It is remarkable that  $(E, \ell)$ -networks with values of  $q$  in the range  $q \in (25, 50)$  produce synchrony-optimized networks of the same synchronization quality as DRA. We stress that this way to construct synchrony-optimized networks is computationally much faster than the DRA algorithm proposed in Ref. 5. To investigate the range of optimal values  $q^*$ , in Figure 10, we plot  $\bar{r}$  as a function of  $q$  measured at fixed values of the coupling strength  $K$ . A comparison with the values of  $\bar{r}$  of the DRA-optimized network reveals that there is no value of  $q$ , which allows for optimal synchronization behaviour at all coupling strengths. In particular, for each value of  $K$ , the curve  $\bar{r}(q)$  has its maximum at different values of  $q$ . We conclude that there is no optimal topological structure valid for all values of  $K$ . We have encountered this already in Figure 4 where for very small values of the coupling strength  $K$ , the  $E$ -minimized network was optimal, whereas for large values of  $K$  it was suboptimal.

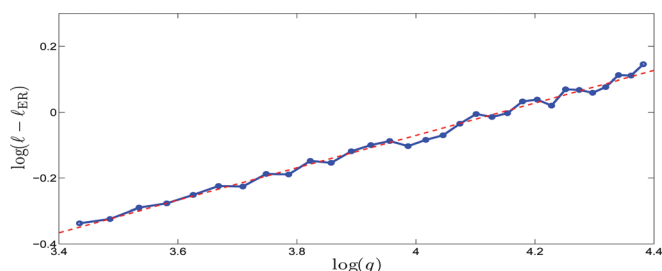


FIG. 8. (Color online) Log-log plot of the average path length  $\ell$  as a function of the rewiring probability  $q$ . The slope of the line of best fit (dashed line) is 0.493.

#### IV. LOCAL SYNCHRONIZATION AT WEAK COUPLING

Synchrony optimized networks clearly exhibit two separate regimes of synchronization for different ranges of  $K$ . For  $K > K_c \approx 18$ , we observe the typical global synchrony branch. For  $K < K_c$ , we observe enhanced synchronization with nonvanishing values of  $\bar{r}(K)$ . Remarkably, we found that the  $\bar{r}$ -curves of all  $E$ -minimized networks ( $q = \infty$ ), which differ in the seed ER used to initialize the optimization, collapse onto the same linear curve for small values of  $K < 12$  (but differ significantly for higher values of  $K$ ). We will now discuss the enhanced synchronizability of synchrony-optimized networks in the local regime for weak coupling strengths  $K$ .

First, recall that networks of minimal  $E$  have a very unusual pairing structure. Nodes of largest  $|\omega_i|$  and opposite sign are likely to be paired together to produce negative energies. Similarly, nodes with  $\omega_i \approx 0$  are likely to be paired to each other in order to minimize  $E$ . Note that rewiring the small  $\omega_i$  nodes does not significantly change the energy  $E$ . We propose that the small-  $|\omega_i|$  communities are causing these networks to register high values of  $\bar{r}$  at weak coupling strengths. The closer the frequencies of adjacent nodes are in value, the smaller is the required critical coupling strength for mutual synchronization. Those communities of nodes with small  $|\omega_i|$  can mutually synchronize at small  $K$  independent of their respective signs, and then act as a stable community of nodes entraining algebraically larger frequencies (recall that  $\langle \omega \rangle = 0$ ). Therefore, synchronized clusters

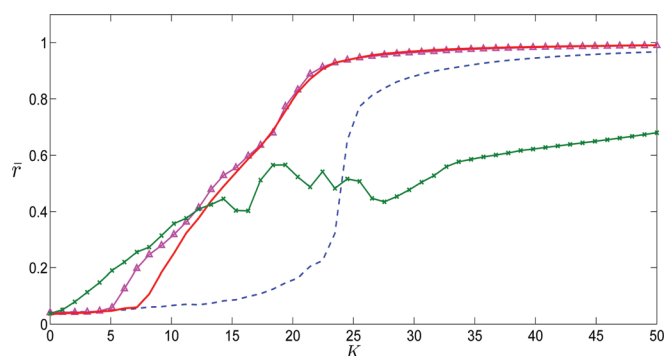


FIG. 9. (Color online) Synchrony order parameter  $\bar{r}$  as a function of coupling strength  $K$  for the  $N = 500$  synchrony-optimized networks. We show a DRA-optimized network (continuous line, online red) and several  $(E, \ell)$ -networks with  $q = 0$  (dashed, online blue),  $q = \infty$  (crosses, online green), and  $q = 30$  (triangles, online magenta). For the energy minimized networks with  $q = 0$ , we have plotted an average over 6 separate networks.

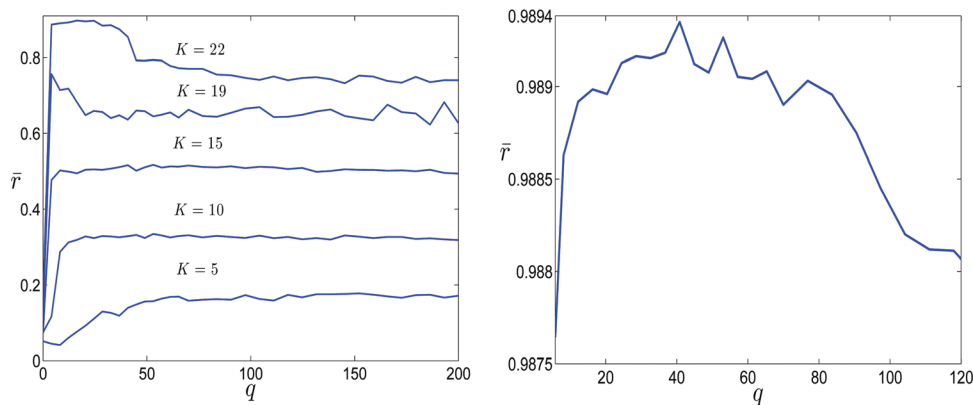


FIG. 10. (Color online) Left: Synchrony order parameter  $\bar{r}$  as a function of the rewiring probability  $q$  for several values of the coupling strength  $K$ . Right: For the coupling strength  $K = 50$ , we present a zoom at low values of  $q$  showing that there exists a value  $q^*$  such that synchronization is maximized.

begin to form in the  $E$ -minimized network at lower coupling strengths than in the DRA network.<sup>29</sup>

### A. Linear scaling of the local synchronization regime for weak coupling

The local regime for synchronization of synchrony-optimized networks exhibits a clear linear growth behaviour as a function of the coupling strength  $K$ , which is clearly visible in Figures 4 and 9. We claim that this linear scaling will occur in highly negative energy networks such as synchrony optimized networks (DRA,  $(E, \ell)$ -networks). This is supported by the following simple argument.

Suppose we have a synchrony-optimized network of  $N$  nodes. Our numerical experiments suggest that there is a synchronized cluster of nodes with small  $|\omega_i|$  even for very low values of  $K$ . Let  $\Gamma_K$  be the set of all nodes in this cluster at coupling strength  $K$ . Clearly,  $\Gamma_K$  will grow with  $K$ , and we wish to know how the size of  $\Gamma_K$  scales with  $K$ . For a node  $i$  to be in  $\Gamma_K$ , its frequency  $\phi_i(t)$  must be locked to the mean frequency, which in our case is zero. From the oscillator dynamics [Eq. (2.1)], we obtain a condition for node  $i$  to be in the locally synchronized cluster  $\Gamma_K$ , given by

$$|\omega_i| = \left| \frac{K}{N} \sum_{j=1}^N a_{ij} \sin(\phi_j - \phi_i) \right| < \frac{K}{N} k_i,$$

for all  $i \in \Gamma_K$ . Here,  $k_i = \sum a_{ij}$  is the degree of node  $i$ . Since the  $E$ -minimized networks have identical degree distributions to the initial ER, the degree of an individual node  $k_i$  does not differ much from the mean degree  $\langle k \rangle$ . This yields the simple requirement for membership in  $\Gamma_K$

$$|\omega_i| < \frac{\langle k \rangle K}{N}.$$

The low energy structure of the synchrony-optimized network ensures that all the nodes with  $|\omega_i|$  small enough to satisfy the above inequality are linked to each other and are found in the small- $|\omega_i|$  community. Therefore, they will readily form a synchronized cluster. We therefore assume that all nodes that can potentially become entrained at coupling strength  $K$  do become entrained. The size of  $\Gamma_K$  is then simply the number of nodes whose absolute values of their native frequencies is smaller than  $K\langle k \rangle/N$ . This is given by

$$|\Gamma_K| = N \int_{|\omega| < \frac{K\langle k \rangle}{N}} g(\omega) d\omega,$$

where  $g(\omega)$  is the probability density function of the native frequencies  $\omega$ . Suppose that  $g$  is sufficiently smooth. A simple Taylor expansion implies that

$$|\Gamma_K| = 2g(0)\langle k \rangle K + \mathcal{O}\left(\frac{\langle k \rangle^2 K^2}{N}\right). \quad (4.1)$$

We may now calculate the order parameter  $r$  for this decomposition as

$$r = \frac{1}{N} \left| \sum_{j \in \Gamma_K} e^{i\phi_j} + \sum_{j \notin \Gamma_K} e^{i\phi_j} \right|.$$

We further assume that all oscillators in  $\Gamma_K$  are locked to the same phase, and all others are randomly distributed. Thus we obtain the linear relationship

$$\begin{aligned} r(K) &= \frac{1}{N} |\Gamma_K| + \mathcal{O}\left(\frac{1}{\sqrt{N}}\right) \\ &= \frac{\langle k \rangle K}{N} + \mathcal{O}\left(\frac{1}{\sqrt{N}}, \frac{K^2 \langle k \rangle^2}{N^2}\right) \\ &= pK + \mathcal{O}\left(\frac{1}{\sqrt{N}}, p^2 K^2, \frac{pK}{N}\right). \end{aligned} \quad (4.2)$$

In the above, we use relation [Eq. (4.1)] and the fact that for ERs we have  $\langle k \rangle = p(N-1)$ . The argument suggests that linear scaling is expected for all  $K \ll 1/p$ , which agrees with all linear behaviour observed thus far.

We test our prediction for the  $N = 500$  node synchrony-optimized network with  $p = 0.05$  and  $g \sim \mathcal{U}(-1, 1)$ , so that  $g(0) = 1/2$ . In Figure 11, we plot  $\bar{r}$  as a function of  $K$  and compare the analytical result [Eq. (4.2)] with results from our synchrony-optimized networks. The actual slope is approximately 30% smaller than the predicted slope, but this is unsurprising given that we took  $\Gamma_K$  to be the theoretically maximal size, and that we further assumed that all oscillators in  $\Gamma_K$  were exactly equal in phase and had equal node degree  $k_i = \langle k \rangle$ . Furthermore, there is a finite size effect due to the sampling of the uniformly distributed native frequencies. We checked that for  $N = 2000$  the slope increases to 0.04.



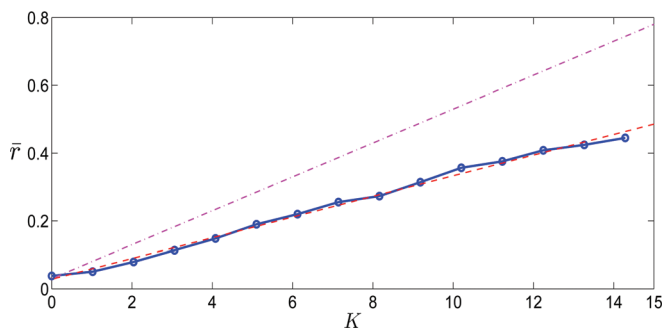


FIG. 11. (Color online) Order parameter  $\bar{r}$  as a function of coupling strength  $K$  for the local synchronization branch for the  $(E, \ell)$ -networks with  $q = \infty$  (continuous line, online blue). The dashed line (online red) shows the best linear fit and the dashed-dotted line (online magenta) shows the predicted linear behaviour [Eq. (4.2)]. For this particular network,  $\langle k \rangle / (N - 1) = 0.05$ . The line of best fit has slope 0.034.

In this section, we have analysed the behaviour of the local synchrony branch. We found that the existence of significant coherence for weak coupling  $K$  is explained by the presence of small- $|\omega_i|$  communities in synchrony-optimized networks. Furthermore, we showed that the linear scaling behaviour in  $\bar{r}$  follows from the simple fact that the size of the small- $|\omega_i|$  synchronized cluster  $\Gamma_K$  grows linearly with  $K$ .

## V. DISCUSSION

We proposed a novel rewiring algorithm aimed at producing synchrony optimized networks of non-identical Kuramoto oscillators with a given fixed degree distribution. The algorithm is built around the observation that, in synchrony optimized networks, there is a high degree of anti-correlation between nodes with native frequencies of similar absolute value but opposite sign. We presented a simple and computationally cheap algorithm to construct networks, which maximize this anti-correlation by minimizing an energy-like quantity  $E$ . However, we found that in order for oscillators to communicate more efficiently in a network, a balance between having small communication length and large anti-correlation between neighbouring frequencies must be achieved. In a second step of the synchrony-optimization algorithm, we therefore rewire the  $E$ -minimized network with a prescribed probability to decrease the average smallest path length  $\ell$ . The resulting  $(E, \ell)$ -minimized networks have very similar synchronization properties as measured by the order parameter  $\bar{r}$  to a dynamically rewired network proposed in Ref. 5. We verified this for a wide range of the rewiring probability  $q$ . This indicates that the two properties of energy and path length are the two dominant properties for network synchronization of ER's with constant degree distribution and non-identical native frequencies. The actual balance between those dominant topological properties depends strongly on the coupling strength. In particular, we found that for large coupling strengths  $K > K_c$ , when the dynamics evolves on the global synchronization branch, the requirement of small average path length is significant, whereas for small coupling strengths  $K < K_c$ , below the onset of global synchronization, the requirement for small average path length seems irrelevant. As in Ref. 22, we find

that particular homogeneity properties are promoted in optimal networks, even when they impose a greater average path length.

The particular topological structure of  $(E, \ell)$ -minimized networks provides several new and atypical phenomena. Interestingly, we identified a local synchronization regime for  $K < K_c$ , where synchrony optimized networks exhibit robust enhanced synchronization behaviour. We have linked this enhanced synchronization to the special topological structure of highly negative energy networks. Networks obtained by minimizing  $E$  have the tendency to pair up oscillators with similar but sign-opposite native frequencies. This creates local communities of oscillators with small algebraic frequencies which—amongst themselves—can synchronize at values of  $K$  way below  $K_c$  required for complete synchronization of the full network. This local synchrony regime is characterized by linear growth of  $\bar{r}$  as a function of  $K$ . We showed that the linear scaling is caused by the presence of a small- $|\omega_i|$  community and derived an approximate formula for this scaling behaviour.

Simulated annealing<sup>18</sup> is a natural algorithm to study the rewiring of networks, which has received recent attention.<sup>8,9</sup> We also used simulated annealing to find the global minimum of the high-dimensional energy landscape  $E$ ,<sup>16</sup> and in order to control the average path length  $\ell$ , we considered a constrained energy introducing a penalty term on  $\ell$ . This procedure is also able to create synchrony-optimized networks,<sup>16</sup> but as DRA simulated annealing is computationally expensive.

It is pertinent to mention that the  $(E, \ell)$ -minimized networks are not necessarily optimized for synchronization (in order to do that one would need to perform optimization with respect to  $\bar{r}$  or  $K_c$ ). If one is simply interested in generating optimized networks, without trying to extract dominant topological features which enhance synchronization, one may want to perform simulated annealing not on some energy-like quantity but on  $\bar{r}$ . This can be done at each coupling strength  $K$ , but would be computationally extremely expensive. We have performed such an optimization of  $\bar{r}$  for  $N = 200$  node networks using simulated annealing.<sup>16</sup> The topological properties and the associated  $\bar{r}(K)$  curve were qualitatively the same as the ones discussed here, showing a linear local synchronization branch as well as enhanced global synchronization. We note that for  $N = 200$  node networks, we did not find a local synchronization branch in DRA-minimized networks.

## ACKNOWLEDGMENTS

We would like to thank Takashi Nishikawa for a critical reading of an earlier version of our manuscript. The research of GAG was supported in part by the Australian Research Council.

<sup>1</sup>Acebrón, J. A., Bonilla, L. L., Pérez Vicente, C. J., Ritort, F., and Spigler, R., "The Kuramoto model: A simple paradigm for synchronization phenomena," *Rev. Mod. Phys.* **77**, 137–185 (2005).

<sup>2</sup>Arenas, A., Díaz-Guilera, A., Kurths, J., Moreno, Y., and Zhou, C., "Synchronization in complex networks," *Phys. Rep.* **469**, 93–153 (2008).

<sup>3</sup>Barrat, A., Barthélemy, M., and Vespignani, A., *Dynamic Processes on Complex Networks* (Cambridge University Press, Cambridge, 2008).

- <sup>4</sup>Boccaletti, S., Latora, V., Moreno, Y., Chavez, M., and Hwang, D. U., "Complex networks: Structure and dynamics," *Phys. Rep.* **424**, 175–308 (2006).
- <sup>5</sup>Brede, M., "Synchrony-optimized networks of non-identical Kuramoto oscillators," *Phys. Lett. A* **372**, 2618–2622 (2008).
- <sup>6</sup>Brede, M., "Local vs. global synchronization in networks of non-identical Kuramoto oscillators," *Eur. Phys. J. B* **62**, 87–94 (2008).
- <sup>7</sup>Cohen, R., and Havlin, S., "Scale free networks are ultrasmall," *Phys. Rev. Lett.* **90**, 058701 (2003).
- <sup>8</sup>Dadashi, M., Barjasteh, I., and Jalili, M., "Rewiring dynamical networks with prescribed degree distribution for enhancing synchronizability," *Chaos* **20**, 043119 (2010).
- <sup>9</sup>Donetti, L., Hurtado, P. I., and Muñoz, M. A., "Entangled networks, synchronization, and optimal network topology," *Phys. Rev. Lett.* **95**, 188701 (2005).
- <sup>10</sup>Lago-Fernandez, L. F., Huerta, R., Corbacho, F., and Sigüenza, J. A., "Fast response and temporal coherent oscillations in small-world networks," *Phys. Rev. Lett.* **84**, 02758 (2000).
- <sup>11</sup>Gómez-Gardeñes, J., Moreno, Y., and Arenas, A., "Paths to synchronization on complex networks," *Phys. Rev. Lett.* **98**, 034101 (2007).
- <sup>12</sup>Gómez-Gardeñes, J., Moreno, Y., and Arenas, A., "Synchronizability determined by coupling strength and topology on complex networks," *Phys. Rev. E* **75**, 066106 (2007).
- <sup>13</sup>Guardiola, X., Díaz-Guilera, A., Llas, M., and Pérez, C. J., "Synchronization, diversity, and topology of networks of integrate and fire oscillators," *Phys. Rev. E* **62**, 5565–5570 (2000).
- <sup>14</sup>Hagberg, A., and Schult, D. A., "Rewiring networks for synchronization," *Chaos* **18**, 037105 (2008).
- <sup>15</sup>Hong, H., Kim, B. J., and Choi, M. Y., "Synchronization on small-world networks," *Phys. Rev. E* **66**, 018101 (2002).
- <sup>16</sup>Kelly, D., "On the topology of synchrony optimized networks," M.Sc Thesis, University of Sydney, 2009.
- <sup>17</sup>Kelly, D. and Gottwald, G. A., "On synchrony optimized Kuramoto networks with non-identical oscillators at low coupling strength," unpublished.
- <sup>18</sup>Kirkpatrick, S., Gelatt, C. D., and Vecchi, M. P., "Optimization by simulated annealing," *Science* **220**, 671–680 (1983).
- <sup>19</sup>Maslov, S., and Sneppen, K., "Specificity and stability in topology of protein networks," *Science* **296**, 910–914 (2002).
- <sup>20</sup>Motter, A. E., Zhou, C., and Kurths, J., "Network synchronization, diffusion, and the paradox of heterogeneity," *Phys. Rev. E* **71**, 016116 (2005).
- <sup>21</sup>Newman, M. E. J., "The structure and function of complex networks," *SIAM Rev.* **45**, 167–256 (2003).
- <sup>22</sup>Nishikawa, T., Motter, A. E., Lai, Y.-C., and Hoppensteadt, F. C., "Heterogeneity in oscillator networks: Are smaller worlds easier to synchronize?" *Phys. Rev. Lett.* **91**, 014101 (2003).
- <sup>23</sup>Pecora, L. M., and Carroll, T. L., "Master stability functions for synchronized coupled systems," *Phys. Rev. Lett.* **80**, 2109–2112 (1998).
- <sup>24</sup>Pikovsky, A., Rosenblum, M., and Kurths, J., *Synchronization: A Universal Concept in Nonlinear Science* (Cambridge University Press, Cambridge, 2001).
- <sup>25</sup>Strogatz, S. H., "From Kuramoto to Crawford: Exploring the onset of synchronization in populations of coupled oscillators," *Physica D* **143**, 1–36 (2000).
- <sup>26</sup>Strogatz, S. H., "Exploring complex networks," *Nature* **410**, 268–276 (2001).
- <sup>27</sup>Strogatz, S. H., and Watts, D. J., "Collective dynamics of 'small-world' networks," *Nature* **393**, 440–443 (1998).
- <sup>28</sup>Zhou, C., and Kurths, J., "Hierarchical synchronization in complex networks with heterogeneous degrees," *Chaos* **18**, 037105 (2008).
- <sup>29</sup>We use the term cluster loosely, to represent a connected subgroup of the network. This is unrelated to the clustering coefficient  $C$ .